Three Modules Modeling of Downdraft Gasification and Influences of Moisture Content and Air to Fuel Ratio

C. Dejtrakulwong[1,2], S. Patumsawad[3,*]

[1]The Joint Graduate School of Energy and Environment, King Mongkut's University of Technology Thonburi, Bangkok 10140, Thailand
[2]Center of Excellence for Energy Technology and Environment, Ministry of Education
[3]Department of Mechanical Engineering, Faculty of Engineering, King Mongkut's University of Technology North Bangkok, Bangkok 10800, Thailand
*Corresponding Author: stt@kmutnb.ac.th

Abstract: From energy and environment problems the renewable energy is attractive to replace the fossil fuel. The biomass downdraft gasification process is interested for clean energy production. The downdraft gasification model was developed to predict the compositions of product gas and also study the effect of operational parameters by considering three modules that consist of equilibrium drying-pyrolysis module, sequence equilibrium oxidation module, and kinetic reduction module. This model was developed by using MATLAB with the iterative Newton-Raphson's numerical method. The main assumptions are: all gases are ideal and pressure is constant. This work focuses the influences of moisture content and air to fuel ratio on temperature and gas composition of each zones by varying from 0 to 40% for moisture content and from 1.4 to 3 for air to fuel ratio. The model validation shows a good agreement with the experimental data. The temperature of all zones decreased with the moisture content increasing while increased with the air to fuel ratio increasing. The calorific value of final product gas increased from 4.39 to 4.79 MJ/Nm^3 along the increasing of moisture content while decreased from 6.71 to 3.48 MJ/Nm^3 along the increasing of air to fuel ratio.

Keywords: Modeling, Downdraft gasification, Equilibrium model, Synthesis gas, Renewable energy.

Introduction

The world energy demand has increased along with the increasing environmental pollution that has been released from fossil fuel usage. In order to deal with both the energy and environmental problems, alternative and renewable energy is needed. Biomass is a renewable energy resource that can be used to replace the fossil fuel. However, some technologies are required to extract energy from the biomass. Gasification is one of the thermo-chemical processes that can be used for converting the solid fuel into combustible gaseous fuel. The gasification process has drawn a lot of attention because it offers higher efficiencies compared to combustion and pyrolysis [1]. This process operates under the sub-stoichiometric condition or limited air supply. In this study, we focus on the downdraft biomass gasification process, a type of the fixed-bed gasifications. The downdraft gasification is a comparatively cheap method of gasification that can produce a product gas with very low tar content because the product gas passes through the hottest zone and breaks down into low molecular weight components [2]. The product gas also has low particulates.

The downdraft biomass gasification comprises four processes which are drying, pyrolysis, oxidation, and reduction. At the beginning of the downdraft gasification, the feedstock with moisture is fed into the top of the downdraft gasifier. Then in the drying process the moisture content in the biomass vaporizes into water vapor. In the pyrolysis zone, the dry biomass decomposes into volatile and char. In the oxidation zone, the oxidation reaction generates heat from the partial combustion with the air injected into this zone. This heat is supplied to the other zones to use in the endothermic reactions. The products of the oxidation zone come into the reduction zone and react by following the reduction reactions to produce final product gas. The product gas, consisting of H_2, CO, and CH_4, is known as synthesis gas which has usable heating value. In order to yield syn gas that generates high calorific value, both the suitable input materials and the suitable parameter values for operating a gasifier are needed, and these parameters can only be estimated from the experimental data. Since conducting experiments cost significant time and money, mathematical models have been developed and used to (1) determine suitable operational parameters, (2) to predict performance of a gasifier, (3) to determine compositions of syn gas, and (4) to study effects of operational parameters.

Many researchers used the equilibrium models and assumed that the downdraft gasifier behaves as one single zone. The global equilibrium gasification models were based on the mass and energy balances. The equilibrium constants of reactions were used to describe the gasification reactions such as Methanation, Water gas primary, and Water gas shift reactions. The residence time of process was assumed to be high enough for the reactions to reach the thermo-chemical equilibrium. Zainal et al. [3] developed the equilibrium model to study the influence of moisture content on the final gas composition and the gas calorific value. Huang et al. [4] fixed the fraction of CH_4 and CO of the gasification model to match the experimental data in two cases: 1) char is completely consumed, and 2) char remains from the reactions. Melgar et al. [5] have studied the thermo-chemical equilibrium model including the parametric study of the relative fuel to air ratio and moisture content on producer gas composition and the process efficiency. Jarungthammachote et al. [6] improved the quality of the model by multiplying a constant to the equilibrium constant such that the amount of final gas species matches the experimental data. Instead of considering the downdraft gasifier as one single zone, the gasification process can be divided into zones (e.g., drying, pyrolysis, oxidation, and reduction zones) inside the gasifier. Ratnadhariya et al. [7] presented the equilibrium model of the pyrolysis process to find the composition of pyrolysis gas by using the Methanation, Water gas primary, and Water gas shift reactions to calculate the equilibrium constant. For the oxidation zone, Sharma [8] proposed the sequence equilibrium model of the oxidation zone by considering the value of the reaction rate of this zone. For the reduction zone, Giltrap et al. [2] have studied a steady state kinetic model with the plentiful char condition and incorporated several factors such as particle size and number of active carbon site into their pre-multiplier called 'Char Reactivity Factor' (CRF), which represents the relative reactivity of different char types. Roy et al. [9-10] and Sharma [11] developed the finite rate kinetic model of the reduction zone with the reduction reactions. The model incorporated the dimension of gasifier which can be used for studying the effects of the gasifier dimensions. In this study the downdraft gasification model was developed by

considering three main modules with the corresponding heat supply from the oxidation module to drying-pyrolysis module to study the gasification process and the influences of moisture content and air to fuel ratio on product composition, temperature of each process, and calorific value of product gas.

Experimental

In this study the model of the downdraft biomass gasification process is divided into three modules which are drying-pyrolysis, oxidation, and reduction. The equilibrium model is applied to the drying-pyrolysis and oxidation modules. The sequence of the oxidation reactions order is considered in the oxidation model. Heat generated from the oxidation process is transferred in order to use in the endothermic drying-pyrolysis process. The corresponding amount of heat was iterative computed until converged. For the reduction zone the kinetic finite rate model was applied and divided into numbers of control volume with the diverged shape. Figure 1 shows the schematic diagram of the downdraft biomass gasification process of this study.

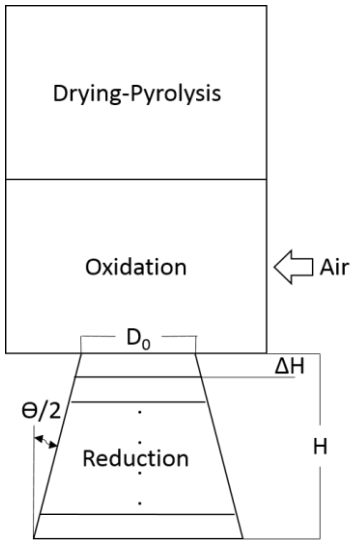

Figure 1. A schematic diagram of the three modules (i.e., drying-pyrolysis, oxidation, and reduction) for the downdraft biomass gasifier used in this study.

Module I: Drying-pyrolysis

When using biomass feedstock ($CH_mO_nN_p$) as an input, the drying pyrolysis reaction can be written as follows:

$$CH_mO_nN_p + wH_2O_{(l)} = x_{p,1}H_2 + x_{p,2}CO + x_{p,3}CO_2 + x_{p,4}H_2O_{(g)} + x_{p,5}CH_4 + x_{p,6}N_2 + x_{p,7}C(char)\,, \quad (1)$$

where *m*, *n*, and *p* are the number of atoms of hydrogen, oxygen, and nitrogen per number of atom of carbon in biomass feedstock respectively. *w* represents the amount of moisture content per mol of biomass feedstock, and this amount can be determined using [3]:

$$w = \frac{MW_F \cdot MC}{MW_W(1 - MC)}\,, \quad (2)$$

where MW_F and MW_W are the molecular weights of fuel and water, respectively. MC is the percentage of moisture content per mol of biomass feedstock. In equation (1), $\{x_{p,1}, x_{p,2}, \ldots x_{p,7}\}$ is the set of unknowns for mass balance. In order to determine these seven unknowns, the mass balances of species and the equilibrium constants of reactions are required by using the following equations:

Carbon balance:
$$1 = x_{p,2} + x_{p,3} + x_{p,5} + x_{p,7}\,, \quad (3)$$

Hydrogen balance:
$$m + 2w = 2x_{p,1} + 2x_{p,4} + 4x_{p,5}\,, \quad (4)$$

Oxygen balance:
$$n + w = x_{p,2} + 2x_{p,3} + x_{p,4}\,, \quad (5)$$

Nitrogen balance:
$$p = 2x_{p,6}\,. \quad (6)$$

The next two equations are obtained from the equilibrium constants of the Water gas shift reaction ($CO + H_2O \leftrightarrow CO_2 + H_2$) and the Methanation reaction ($C + 2H_2 \leftrightarrow CH_4$) which CH_4 was assumed to form only via Methanation reaction at char surface. These reactions were assumed that they occurred at the end of this module, where received the energy from oxidation module as flaming pyrolysis to form products. These equilibrium constants are simply the fraction of product to reactant of the reactions. Note that the equilibrium model assumes that all gases are ideal and that there is enough time to reach the thermal and chemical equilibrium. The equilibrium constants of the Water gas shift (K_1) and the Methanation reactions (K_2) are written as:

$$K_1 = \frac{x_{p,1}x_{p,3}}{x_{p,2}x_{p,4}}\,, \quad (7)$$

$$K_2 = \frac{x_{p,5}}{{x_{p,1}}^2}x_{total}\,. \quad (8)$$

The values of the equilibrium constants can be computed from the change of Gibbs function of formation of gas species as a function of temperature (T) which can be expressed as [6]:

$$K_1 = \exp\left(\frac{-\bar{g}^0_{CO_2} - \bar{g}^0_{H_2} + \bar{g}^0_{CO} + \bar{g}^0_{H_2O}}{R_uT}\right), \quad (9)$$

$$K_2 = \exp\left(\frac{-\bar{g}^0_{CH_4} + 2\bar{g}^0_{H_2}}{R_uT}\right), \quad (10)$$

$$\bar{g}^0_i = h^0_f - a'Tln(T) - b'T^2 - \left(\frac{c'}{2}\right)T^3 - \left(\frac{d'}{3}\right)T^4 + \left(\frac{e'}{2T}\right) + f' + g'T, \quad (11)$$

where R_u is the universal gas constant, 8.314 J/(mol·K). h°_f represents the enthalpy of formation of the gases at one atmospheric pressure (i.e., 1 atm) and room temperature (i.e., 298 K), and the coefficient *a'*-*g'* values are shown in the Table 1.

Table 1. The values of h°_f (kJ/mol) and the coefficients of the empirical equation for $\Delta\bar{g}^\circ_{f,T}$ (kJ/mol) [6].

Species	h°_f	*a'*	*b'*	*c'*	*d'*	*e'*	*f'*	*g'*
CO	-110.5	5.619×10^{-3}	-1.190×10^{-5}	6.383×10^{-9}	-1.846×10^{-12}	-4.891×10^{2}	8.684×10^{-1}	-6.131×10^{-2}
CO_2	-393.5	-1.949×10^{-2}	3.122×10^{-5}	-2.448×10^{-8}	6.946×10^{-12}	-4.891×10^{2}	5.270	-1.207×10^{-1}
H_2O	-241.8	-8.950×10^{-3}	-3.672×10^{-6}	5.209×10^{-9}	-1.478×10^{-12}	0.0	2.868	-1.722×10^{-2}
CH_4	-74.8	-4.620×10^{-2}	1.130×10^{-5}	1.319×10^{-8}	-6.647×10^{-12}	-4.891×10^{2}	1.411×10^{1}	-2.234×10^{-1}

The remaining equation obtained from the char yield of biomass feedstock that is divided into char and methane by assuming that methane is formed only on the char surface [9]. This equation is shown as [9]:

$$x_{p,5} + x_{p,7} = \frac{FC}{C}\,, \tag{12}$$

where *FC* and *C* are the fixed carbon from the proximate analysis and carbon from the ultimate analysis in mass percentage, respectively.

The equilibrium temperature of the drying-pyrolysis zone (T_p) is determined based on the energy balance equation which integrates the heat supplied from the oxidation process (Q_{in}). The energy balance can be expressed as:

$$h^{\circ}_{f,fuel} + wh^{\circ}_{f,H_2O_{(L)}} + wh_{vap} + Q_{in} + Q_{loss} = \sum_{i=1}^{6} x_{p,i}\left[h^{\circ}_{f,p,i} + \int_{T_0}^{T_p} \bar{C}_{p,p,i}dT\right] + x_{c,7}\bar{C}_{p,C}\left(T_p - T_0\right), \tag{13}$$

where $h^{\circ}_{f,fuel}$, $h^{\circ}_{f,H_2O_{(L)}}$, and $h^{\circ}_{f,p,i}$ are the enthalpy of formation of fuel, moisture content, and gas species *i* (*i* ranges from 1 to 6 for H_2, CO, CO_2, H_2O, CH_4, and N_2). The specific heat of gas species *i* is the function of temperature [6]: $\bar{C}_{p,p,i}(T) = a + bT + cT^2 + dT^3$. The values of a, b, c, and d are shown in Table 2. $\bar{C}_{p,C}$ is the specific heat of char, 23.4 J/(mol·K) [9]. T_0 is the reference temperature at 298 K. The assumptions of equilibrium model are: all gases are ideal and there is enough residence time to reach the thermo-chemical equilibriums. The Newton Raphson numerical method is used to solve the product composition and equilibrium temperature of the drying-pyrolysis module.

Module II: Oxidation

In the oxidation zone, a sequence of reactions is considered as follows [12-13]:

$$H_2 + \frac{1}{2}O_2 \rightarrow H_2O\,, \tag{14}$$

$$CO + \frac{1}{2}O_2 \rightarrow CO_2\,, \tag{15}$$

$$CH_4 + \frac{3}{2}O_2 \rightarrow CO + 2H_2O\,, \tag{16}$$

$$\Omega_{comb}C + O_2 \rightarrow 2(\Omega_{comb} - 1)CO + (2 - \Omega_{comb})CO_2\,,$$

$$\Omega_{comb} = \frac{2(1 + 4.3exp[-3390/T_s])}{2 + 4.3exp[-3390/T_s]}\,. \tag{17}$$

These homogeneous and heterogeneous reactions as Eq. (14)–(17) are arranged in decreasing order of their estimated reaction rates. This sequence of reactions indicates the order of reactions in which oxygen firstly react with (e.g., with hydrogen, carbon monoxide, and methane, respectively). The remaining oxygen from the homogeneous reactions reacts with the char following Eq. (17) to produce carbon dioxide and carbon monoxide. The products of the oxidation reactions from Eq. (14)–(17) and the products of the pyrolysis zone that do not react with oxygen become the reactants of the equilibrium model of the oxidation zone:

$$x_{p,1}H_2 + x_{p,2}CO + x_{p,3}CO_2 + x_{p,4}H_2O + x_{p,5}CH_4 + x_{p,6}N_2 + x_{p,7}C_{(S)} + a(O_2 + 3.76N_2) = x_{c,1}H_2 + x_{c,2}CO + x_{c,3}CO_2 + x_{c,4}H_2O + x_{c,5}CH_4 + x_{c,6}N_2 + x_{c,7}C_{(S)}\,, \tag{18}$$

where *a* is the amount of the air injected into the gasifier per mol of biomass feedstock. In Eq. (18), the value of $x_{c,6}$ is already known because nitrogen does not participate in any reaction; it only dilutes the final gas composition [2]. However, $\{x_{c,1}, x_{c,2}, x_{c,3}, x_{c,4}, x_{c,5} x_{c,7}\}$ is the set of unknowns for mass balance. In order to determine these six unknowns, the mass balances of species of the equilibrium reaction as Eq. (18) and the equilibrium constant of the Water gas shift reaction are required by following steps similar to the drying-pyrolysis zone because this reaction can be safely applied for fuel-rich combustion [8, 14]. The computation of the six unknowns is done under the assumptions that methane and char do not react in the Water gas shift reaction and that methane and char pass through to the reduction zone.

The energy balance equation is developed to calculate the equilibrium temperature of the oxidation zone. Note that this energy balance also incorporates heat transferred from the oxidation zone to the drying-pyrolysis zone. The energy balance equation of the oxidation zone can be expressed as follows:

$$\sum_{i=1}^{6} x_{p,i}\left[h^{\circ}_{f,p,i} + \int_{T_0}^{T_p} \bar{C}_{p,p,i}dT\right] + a\int_{T_0}^{T_p} \bar{C}_{p,O_2}dT + 3.76a\int_{T_0}^{T_p} \bar{C}_{p,N_2}dT + x_{p,7}\bar{C}_{p,C}\left(T_p - T_0\right) + Q_{Loss} = \sum_{i=1}^{6} x_{ci}\left[h^{\circ}_{f,c,i} + \int_{T_0}^{T_c} \bar{C}_{p,c,i}dT\right] + x_{c,7}\bar{C}_{p,C}(T_c - T_0) + m_{ash}C_{p,ash}(T_c - T_0) + Q_{supply}, \tag{19}$$

where $h^{\circ}_{f,i}$ is the enthalpy of formation of gas species (iranges from 1 to 6; the number corresponds to H_2, CO, CO_2, H_2O, CH_4, and N_2, respectively). Q_{Loss} is the energy loss from the reactor to the surrounding, and Q_{supply} is the energy supplied to the drying-pyrolysis zone. m_{ash} is the mass flow rate of ash that can be expressed as [9]: $m_{ash} = \frac{m_F ASH}{100}$; m_F represents the mass flow rate of the biomass feedstock, (g/s), and *ASH* is the percentage of ash from the proximate analysis data on dry basis. $C_{p,ash}$ is the specific heat of ash which is assumed to be a constant of 0.84 J/(g·K) [10]. The oxidation model can be calculated same as the drying-pyrolysis zone. The Q_{supply} from the oxidation zone must equal to Q_{in} from the drying-pyrolysis zone. Therefore, the model of both zones is iteratively calculated until the corresponding heat supply was determined.

Table 2. The values of the coefficients for determining the specific heat of gas species [6].

Gas species	*a*	*b*	*c*	*d*	Temperature Range (K)
H_2	29.11	-0.1916×10^{-2}	0.4003×10^{-5}	-0.8704×10^{-9}	273-1800
CO	28.16	0.1675×10^{-2}	0.5372×10^{-5}	-2.222×10^{-9}	273-1800
CO_2	22.26	5.981×10^{-2}	-3.501×10^{-5}	-7.469×10^{-9}	273-1800
$H_2O_{(g)}$	32.24	0.1923×10^{-2}	1.055×10^{-5}	-3.595×10^{-9}	273-1800
CH_4	19.89	5.204×10^{-2}	1.269×10^{-5}	-11.01×10^{-9}	273-1500
N_2	28.90	-0.1571×10^{-2}	0.8081×10^{-5}	-2.873×10^{-9}	273-1800

Module III: Reduction

In the reduction module, the kinetic finite rate model is applied. The assumptions related to the model are that all gas species obey the ideal gas law and that the fixed carbon presented in the biomass feedstock has molecular weight similar to that of carbon. The products formed in the oxidation zone involve in the kinetically controlled chemical reactions in this reduction zone which produce the final gaseous product. The ash from the oxidation zone is also considered in this study. There are four reduction reactions considered in the reduction zone: the Boudouard reaction (Reaction 1: C + CO_2 ↔ 2CO), the Water gas primary reaction (Reaction 2: C + H_2O ↔ CO + H_2), the Methanation reaction (Reaction 3: C + 2H_2 ↔ CH_4), and the Steam reforming reaction (Reaction 4: CH_4 + H_2O ↔ CO + 3H_2). The reaction rates for these four reactions are expressed using Arrhenius equations with the pre-exponential factor (A_R) and activation energy (E_R). The reaction rates of the reduction reactions are evaluated from the forward reactions and the equilibrium constants of the reactions. The rates of reaction of each reaction can be expressed as follows [9]:

$$r_{R1} = C_{RF}A_{R1}exp\left(\frac{-E_{R1}}{\bar{R}T}\right)\left(y_{CO_2} - \frac{y_{CO}^2}{K_{R1}}\right), \quad (20)$$

$$r_{R2} = C_{RF}A_{R2}exp\left(\frac{-E_{R2}}{\bar{R}T}\right)\left(y_{H_2O} - \frac{y_{CO}y_{H_2}}{K_{R2}}\right), \quad (21)$$

$$r_{R3} = C_{RF}A_{R3}exp\left(\frac{-E_{R3}}{\bar{R}T}\right)\left(y_{H_2}^2 - \frac{y_{CH_4}}{K_{R3}}\right), \quad (22)$$

$$r_{R4} = C_{RF}A_{R4}exp\left(\frac{-E_{R4}}{\bar{R}T}\right)\left(y_{H_2O}y_{CH_4} - \frac{y_{H_2}^3 y_{CO}}{K_{R4}}\right), \quad (23)$$

where C_{RF} represents the char reactivity factor that accounts for the active sites present on the char surface [2]. Roy et al. [9] compared the temperature profile of the model against the experimental results of Jayah et al. [15] and they found that using C_{RF} = 100 give the best match between the model and the experiment results. y_i represents the mole fraction of gas species. Values of A_R and E_R for reactions R1 – R4 are shown in Table 3.

Table 3. The values of the pre-exponential factor (A_R) and activation energy (E_R) for the four reduction reactions [16].

Reaction *i*	A_{Ri} (1/s)	E_{Ri} (J/mol)
1	3.616 x 10^1	77,390
2	1.517 x 10^4	121,620
3	4.189 x 10^{-3}	19,210
4	7.301 x 10^{-2}	36,150

The equilibrium constants of the four reactions (R1 – R4) or the change of Gibbs of formation can be determined using the equations as follows:

$$K_{R1} = exp\left(\frac{-2\Delta g_{CO}^{\circ} + \Delta g_{CO_2}^{\circ}}{\bar{R}T}\right), \quad (24)$$

$$K_{R2} = exp\left(\frac{-\Delta g_{CO}^{\circ} - \Delta g_{H_2}^{\circ} + \Delta g_{H_2O}^{\circ}}{\bar{R}T}\right), \quad (25)$$

$$K_{R3} = exp\left(\frac{-\Delta g_{CH_4}^{\circ} + 2\Delta g_{H_2}^{\circ}}{\bar{R}T}\right), \quad (26)$$

$$K_{R4} = exp\left(\frac{-\Delta g_{CO}^{\circ} - 3\Delta g_{H_2}^{\circ} + \Delta g_{CH_4}^{\circ} + \Delta g_{H_2O}^{\circ}}{\bar{R}T}\right). \quad (27)$$

The flow rate (mol/s) of each species *i* (*i* ranges from 1 to 7; the number corresponds to H_2, CO, CO_2, H_2O, CH_4, N_2 and char, respectively) at the entry of the reduction zone can be calculated using [9-10]

$$X_i^0 = \frac{m_F(1 - ASH/100)}{MW_F}x_{c,i}\,, \quad i = \{1, 2, \dots, 7\} \quad (28)$$

The geometry of the reduction zone is considered to be a diverging shape (i.e., truncated cone) with a divergent angle, and this zone is divided into several control volumes as shown in Figure 1. Each control volume *k* has a finite rate of balance of the species *i* which is related the net rate of the reduction reactions can be written as [9-10]:

$$X_i^k = X_i^{k-1} + R_i^k \Delta V_k, \quad (29)$$

where R_i^k represents the net rate of formation of species *i* in the *k*th control volume. ΔV_k is the volume of the respective control volume. Note: considering all the four reactions R1 – R4, if a species appears as a reactant (or a product) in the reaction, the corresponding reaction rate for this species has a negative (or positive) sign. Net reaction rates of formation for various species are shown in Table 4.

Table 4. Net rate of formation of different species per unit volume in terms of the rates of reactions R1 – R4.

Species	R_i (mol/(m^3·s))
H_2	r_{R2} - 2r_{R3} + 3r_{R4}
CO	2r_{R1} + r_{R2} + r_{R4}
CO_2	- r_{R1}
H_2O	- r_{R2} - r_{R4}
CH_4	r_{R3} - r_{R4}
N_2	0
C	- r_{R1} - r_{R2} - r_{R3}

The reduction temperature of the control volume *k* can be determined by using the energy balance across the control volume:

$$\sum_{i=1}^{6} X_i^{k-1}\left[h_{f,i}^{\circ} + \int_{T_0}^{T^{k-1}} \bar{C}_{p,i}dT\right] + X_7^{k-1}\bar{C}_{p,C}(T^{k-1} - T_0) + m_{ash}C_{p,ash}(T^{k-1} - T_0) = \sum_{i=1}^{6} X_i^{k}\left[h_{f,i}^{\circ} + \int_{T_0}^{T^{k}} \bar{C}_{p,i}dT\right] + X_7^{k}\bar{C}_{p,C}(T^{k} - T_0) + m_{ash}C_{p,ash}(T^{k} - T_0)\,. \quad (30)$$

The heat transfer in each control volume was found that has so little effect on the temperature which it can be negligible.

Calculation Procedure

To compute the product compositions and equilibrium temperature of drying-pyrolysis module the initial temperature was assumed and substituted into Eqs. (9) and (10) to calculate the equilibrium constants for using in Eqs. (7) and (8). The product composition can be determined from Eqs. (3)-(8), and (12) by using Newton Rahpson numerical method. Then Eq. (13) was used to solve the new temperature. The drying-pyrolysis module was continuously computed until the temperature converged to get the equilibrium temperature and product composition at this temperature as well. The results of drying-pyrolysis module come into oxidation module as the reactants. In the oxidation module, the oxygen was reacted under the oxidation reactions Eqs. (14)-(17) following the order of reaction rates of each reaction. If oxygen remains from Eq. (14) it will next reacts for Eq. (15), then Eq. (16) and Eq. (17) until the oxygen is completely consumed. Then the products of oxidation process were determined same as the drying-pyrolysis module following Eq. (18). The temperature of this module can be also obtained from Eq. (19) similar method to the drying-pyrolysis module. The supply heat as Q_{supply} for oxidation and Q_{in} for drying-pyrolysis was

iteratively computed until this heat corresponded to both modules which temperature of both modules will also change until converged with the corresponding supply heat. Then, the results of oxidation module came into the reduction module as the initial conditions. Eqs. (24)-(27) were used for calculating the equilibrium constants to determine the reaction rates of Eqs. (20)-(23). The concentration of oxidation products were converted unit from mol to mol/s in Eq. (28) and Eq. (29) was used to compute the mol flow rate of each compositions of control volume *k*. The temperature of control volume *k* can be obtained from Eq. (30). The calculation procedure was shown in Figure 2. The related variable parameters for model validation are air to fuel ratio (A/F) and moisture content (MC).

Results and Discussion

For the model validation, rubber wood was used in this study which the values of feedstock parameters including the high heating value of feedstock that are used in the model calculation are shown in Table 5. Table 6 shows the dimension of the reduction zone of the gasifier about diameter, height, and diverged angle that was used in reference (experiment data). The results of the gasification model in this study is validated against the experimental data from Jayah et al. [15] on the final gas compositions (H_2, CO, CO_2, CH_4, and N_2) by mol fraction (%dry basis) as shown in Figures 3 and 4.

Table 5. The feedstock parameters of rubber wood for the model validation [15].

Proximate analysis (%dry basis)	
Fixed carbon	80.1
Volatile matter	19.2
Ash content	0.7
Ultimate analysis (%dry basis)	
C	50.6
H	6.5
O	42
N	0.2
Ash	0.7
HHV	19,600 kJ/kg

Table 6. The dimension of the reduction zone of the downdraft gasifier with the diverged shape [15].

Dimension of reduction zone	
D_o(m)	0.10
Θ (º)	61
H (m)	0.22

Figures 3 and 4 show a good agreement between the model prediction and the experimental data [15] on the final gas mol fraction (%dry basis) with the conditions of A/F = 2.2, MC = 16% and A/F = 2.37, MC = 14.7% respectively. In the first condition (A/F = 2.2, MC = 16%), the amount of model prediction mol fraction on dry basis of H_2, CO, CO_2, CH_4, and N_2 are 18.44, 18.80, 11.36, 0.53, and 50.87% respectively while experiment data showed 18.3, 20.2, 9.7, 1.1, and 50.7% respectively. The amount of CO and CH_4 of the model are lower than the experimental data while the amount of CO_2 is higher. However, the amounts of H_2 and N_2 are close to the experimental data. For the second condition (A/F=2.37, MC=14.7%), the amount of H_2, CO, and CO_2 from the model prediction are 18.20, 19.79, and 10.65% which are higher than the experimental data that are 17.2, 19.4, and 9.7% for H_2, CO, and CO_2 respectively and the amount of CH_4 and N_2 are lower than the experimental data as shown in Figure 4.

For the parametric study of moisture content, air to fuel ratio was fixed at 2.2 and moisture content was varied from 0 to 40%. The moisture content increasing from 0 to 40% resulted the temperature decreasing from 1221.77 to 946.13 K for drying-pyrolysis zone, from 1544.69 to 1364.74 K for oxidation zone, and from 1269.06 to 1181.11 K for reduction zone because they need more heat to vaporize moisture content in feedstock to water vapor. Figure 5 shows the temperatures of drying-pyrolysis, oxidation, and reduction zones with the moisture content varying which temperature of all zones have decreasing trends.

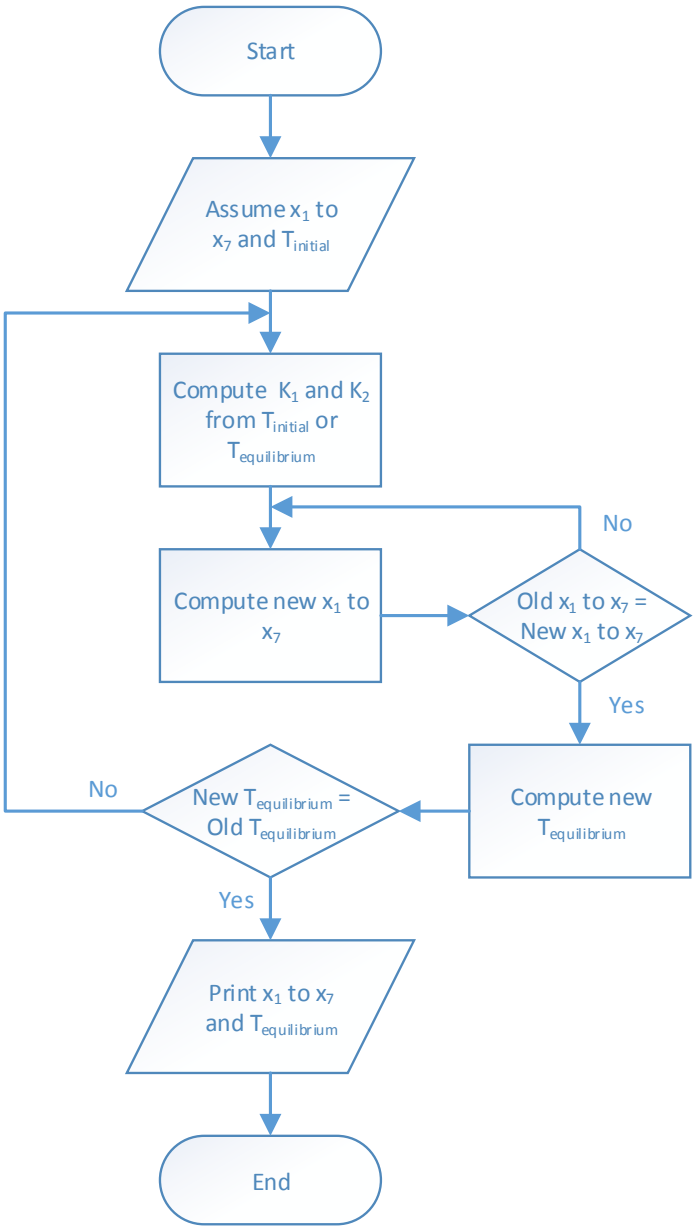

Figure 2. Calculation procedure of this model.

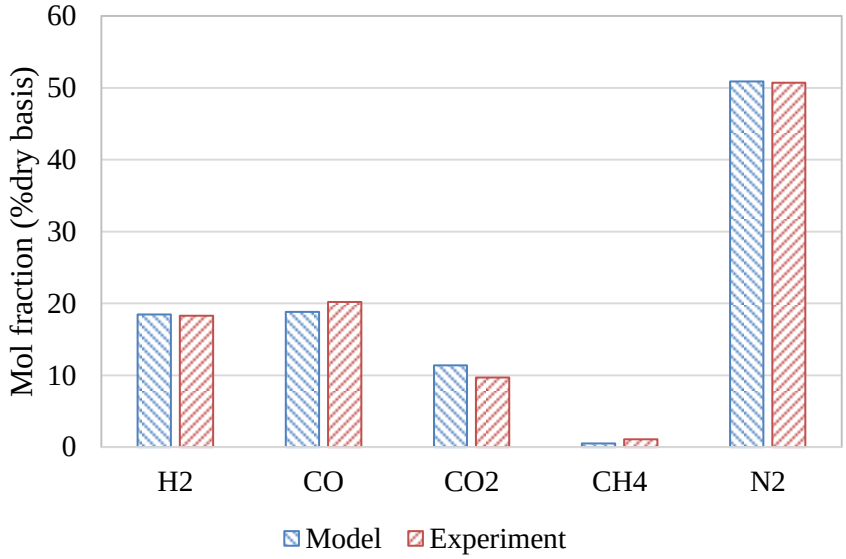

Figure 3. Comparison between the model prediction and the experimental data [15] on the final gas compositions (%dry basis) of rubber wood with the condition of A/F = 2.2, MC = 16%.

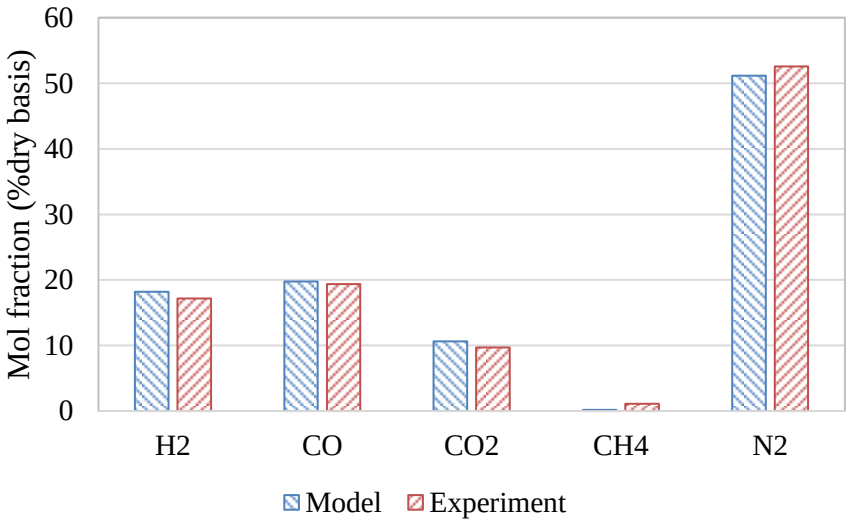

Figure 4. Comparison between the model prediction and the experimental data [15] on the final gas compositions (%dry basis) of rubber wood with the condition of A/F = 2.37, MC = 14.7%.

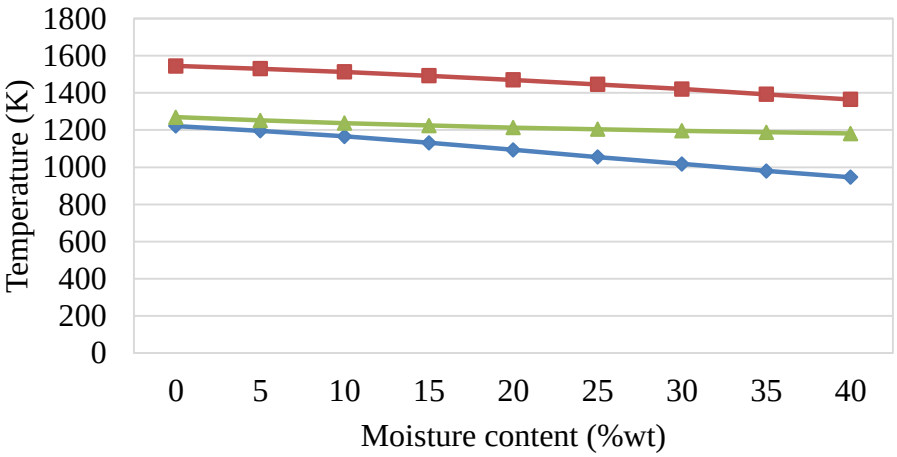

Figure 5. Temperature of drying-pyrolysis, oxidation, and reduction modules with the moisture content varying. T_p (◆), T_c (■), T_r (▲).

Figures 6 to 8 show the gas compositions on mol fraction (%wet basis) of drying-pyrolysis, oxidation, and reduction zones with the moisture content varying. For the drying-pyrolysis module, the two reactions of this module more occurred because the water vapor as reactant of the Water gas shift reaction is more that directly related the amount of H_2 as the reactant of Methanation reaction. So, the amount of H_2 slightly decreased from 54.48 to 39.88% and the amount of CO decreased from 44.73 to 13.06% with the moisture content increasing from 0 to 40% while CO_2, CH_4 and H_2O sharply increased from 0.05 to 14.99%, 0.52 to 4.94%, and 0.09 to 27.04% respectively. For the oxidation module, the amounts of CH_4 and CO_2 increased from 0.25 to 2.36% and 9.47 to 10.70% respectively but H_2 and CO decreased from 7.91 to 5.34% and 12.02 to 2.67% respectively with the moisture content increasing due to the temperature of oxidation zone dropping and the water gas shift more occurring with the moisture content increasing. For the reduction module, the gas compositions trends are similar to the oxidation module because the fraction of water vapor is high and the endothermic reactions of reduction module less occurred with the temperature decreasing. The amount of H_2 decreased from 14.35 to 10.54% and CO also decreased 19.06 to 8.15% while CH_4 increased from 0.19 to 2.09% with the moisture content increasing. Figure 9 shows the calorific value of the final product gas on dry basis slightly increasing from 4.39 to 4.79 MJ/Nm^3 along the moisture content increasing mainly from the increasing of H_2 from Water gas shift reaction and CH_4 was consequentially produced following to Methanation reaction from the increasing of H_2.

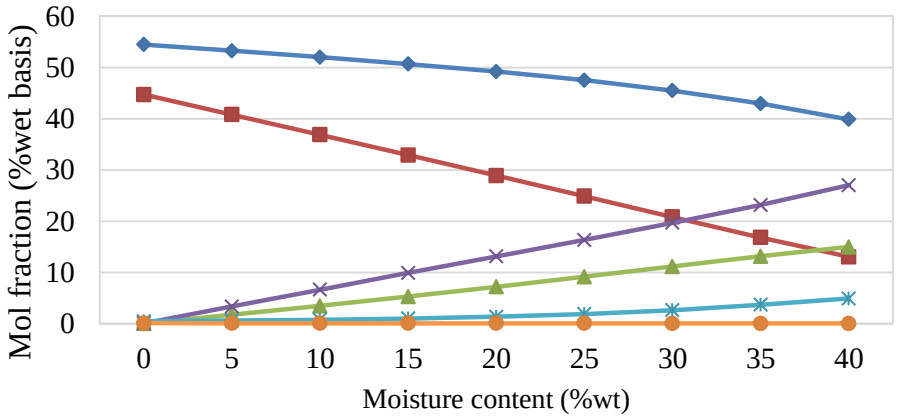

Figure 6. Gas compositions of drying-pyrolysis module on mol fraction (%wet basis) with the moisture content varying. H_2 (◆), CO (■), CO_2 (▲), H_2O (×), CH_4 (✳), N_2 (●)

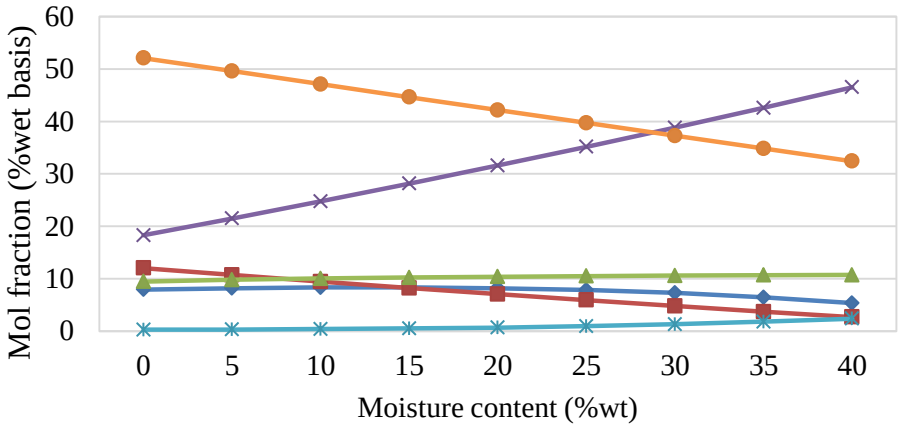

Figure 7. Gas compositions of oxidation module on mol fraction (%wet basis) with the moisture content varying. H_2 (◆), CO (■), CO_2 (▲), H_2O (×), CH_4 (✳), N_2 (●)

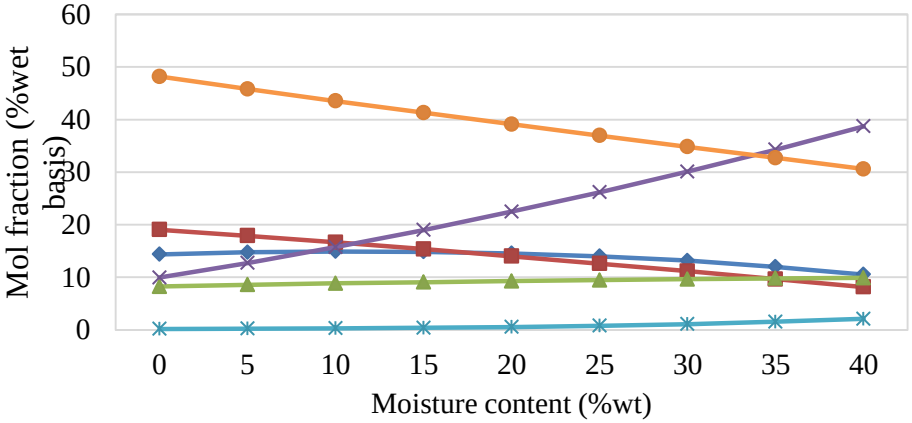

Figure 8. Gas compositions of reduction module on mol fraction (%wet basis) with the moisture content varying. H_2 (◆), CO (■), CO_2 (▲), H_2O (×), CH_4 (✳), N_2 (●)

For the influence of air to fuel ratio study, moisture content was fixed at 16% and air to fuel ratio was varied from 1.4 to 3. The increasing of air to fuel ratio resulted the increasing of air injecting into the gasifier which directly affects the temperature of gasifier increasing from oxidation reactions. Figure 10 shows the temperatures of drying-pyrolysis, oxidation, and reduction zones increasing from 819.64, 1229.75, and 1135.55 K to 1657.34, 1871.12, and 1521.66 K respectively with the air to fuel ratio varying from 1.4 to 3. For the drying-pyrolysis module, the amounts of H_2 and CO increased from 37.34 and 29.43% to 49.07 and 34.66% respectively with the air to fuel ratio increasing while CO_2 and CH_4 decreased from 13.48 to 2.79% and 14.65 to 0.06% respectively due to the reactions of pyrolysis zone as Water gas shift and Methanation reactions from above assumption less occurring from the increasing of oxidation reaction that supplied more useful heat energy to drying-pyrolysis zone as shown in Figure 11. Figure 12 shows the gas compositions of oxidation zone on mol fraction (%wet basis) with the air to fuel ratio varying which the amounts of H_2, CO, and CH_4 decreased because the oxidation reactions more occurred. N_2 sharply increased along A/F increasing as more air supply which N_2 did not react to others to form nitrogen oxide products. The amount of CO_2 seemed to decrease from the sharply increasing of N_2. Figure 13 shows the gas compositions of reduction zone on mol fraction (%wet basis) with the air to fuel ratio varying which the reduction reactions more occurred with the increasing of temperature. So, the amount of CH_4 sharply decreased from 7.28 to 0.02% while H_2 and CO increased with air to fuel ratio of 1.4 to 2.4 and then decreased along air to fuel ratio of 2.4 to 3. The calorific value of final gas with the air to fuel ratio varying is shown in Figure 14. The calorific value is the decreasing trend from 6.71 to 3.48 due to the sharply decreasing of CH_4.

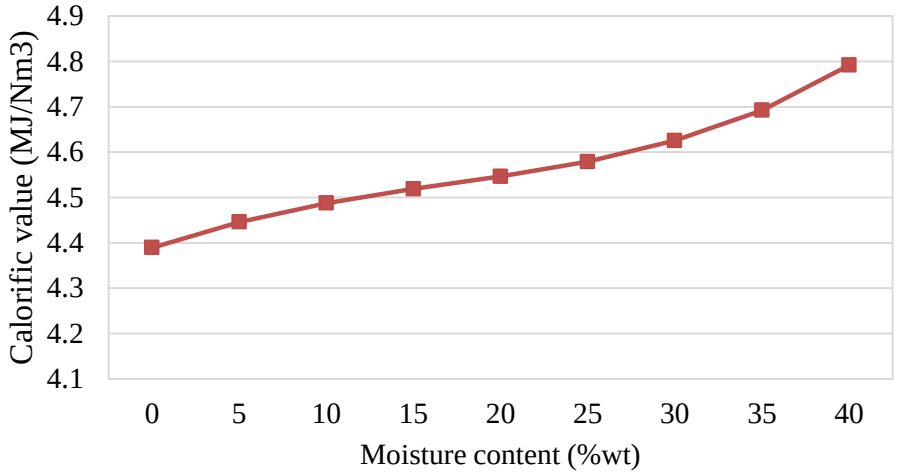

Figure 9. Calorific value of final gas product with the moisture content varying.

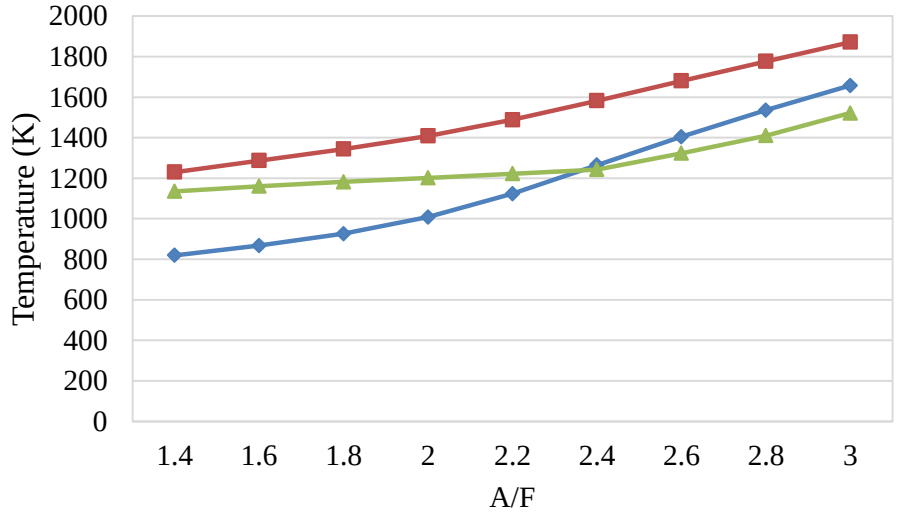

Figure 10. Temperature of drying-pyrolysis, oxidation, and reduction modules with the air to fuel ratio varying. T_p (◆), T_c (■), T_r (▲).

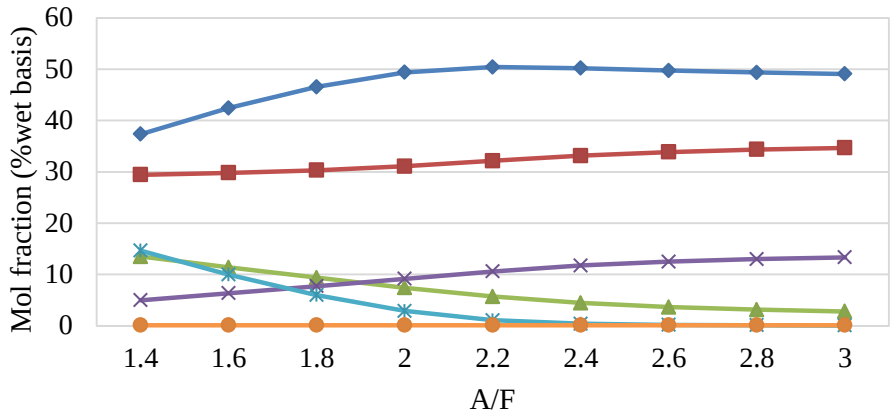

Figure 11. Gas compositions of drying-pyrolysis module on mol fraction (%wet basis) with the air to fuel ratio varying. H_2 (◆), CO (■), CO_2 (▲), H_2O (×), CH_4 (✳), N_2 (●)

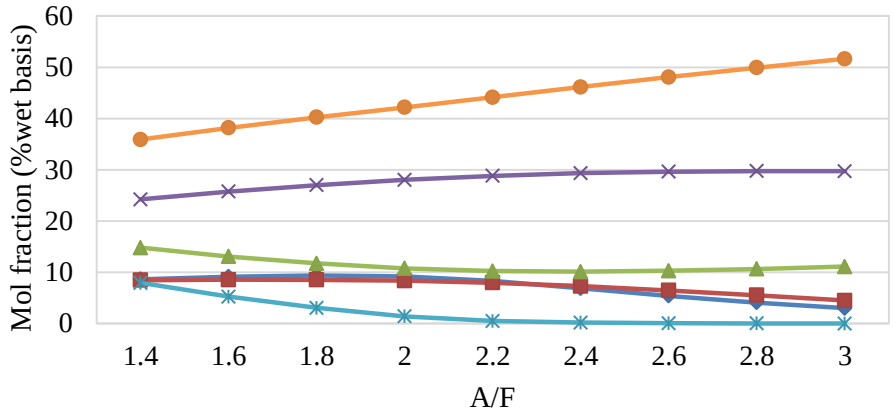

Figure 12. Gas compositions of oxidation module on mol fraction (%wet basis) with the air to fuel ratio varying. H_2 (◆), CO (■), CO_2 (▲), H_2O (×), CH_4 (✳), N_2 (●)

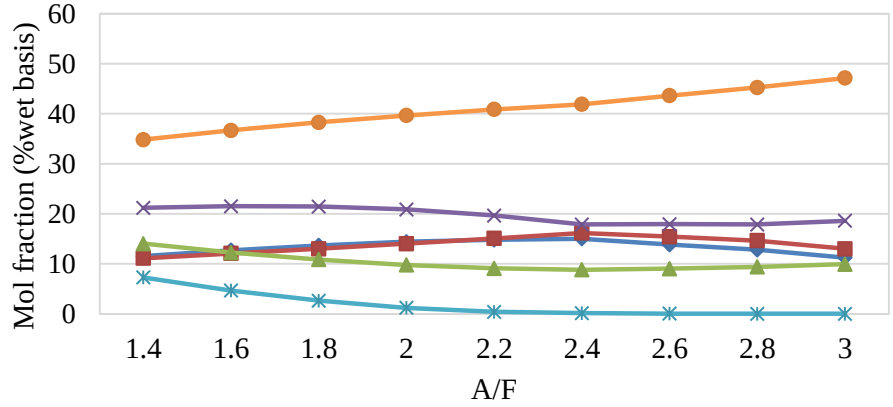

Figure 13. Gas compositions of reduction module on mol fraction (%wet basis) with the air to fuel ratio varying. H_2 (◆), CO (■), CO_2 (▲), H_2O (×), CH_4 (✳), N_2 (●)

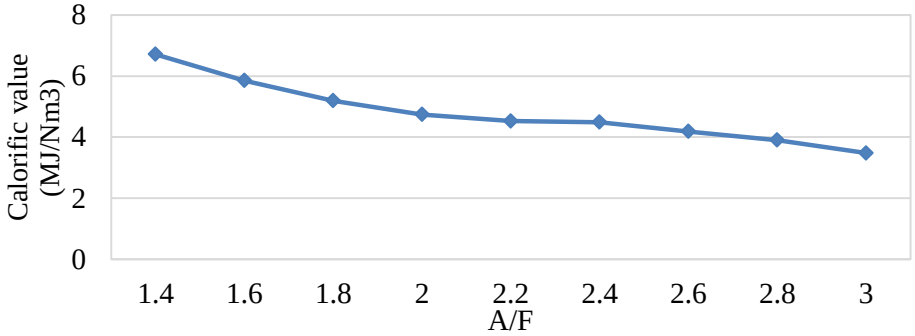

Figure 14. Calorific value of final gas product with the air to fuel ratio varying.

Conclusions

The downdraft gasification model was developed by considering three modules which are drying-pyrolysis, oxidation, and reduction based on mass and energy balances. The integration of the drying and the pyrolysis zones was developed by using the equilibrium model with the char yield of feedstock equation. The products of the drying-pyrolysis zone came into the oxidation zone where air is injected to promote thZe oxidation reactions. The sequence of oxidation reactions was determined by the rate of oxidation reactions at the reaction temperature. The heat from the partial oxidation supplied to the drying-pyrolysis zone which the model was iterative calculated the corresponding amount of supply heat. The equilibrium temperatures of drying-pyrolysis and oxidation zones were then determined to find the product compositions. The equilibrium temperature and products of oxidation module passed the reduction process with the four reduction reactions. The reduction zone was considered to be diverged shape with the numbers of control volume. The final gas compositions of reduction zone were compared to the experimental results for validating the three modules gasification model on percentages of mol fraction (dry basis). The comparison of model predictions shows good agreement with the experimental data.

The moisture content increasing directly resulted the decreasing of temperature of gasifier because it need more heat to vaporize moisture content in the feedstock to water vapor which the water gas shift reaction more occurred while the endothermic reactions of reduction module less occurred. For the effect of air to fuel ratio, the temperature of gasifier increased with the air to fuel ratio increasing because air is more injected into oxidation zone and oxidation reactions as exothermic reactions more occurred. The water gas shift reaction less occurred while the endothermic reactions of reduction module more occurred with the air to fuel ratio increasing. The calorific value on dry basis increased with the moisture content increasing but decreased with the air to fuel ratio increasing. The results of this study can be used to study the behavior of the gasification process.

Acknowledgements

I would like to thank JGSEE for the financial supports, and my advisor and committee for the research advices.

References

[1] Babu BV, Sheth PN, Modeling and simulation of reduction zone of downdraft biomass gasifier: Effect of char reactivity factor, *Energy Conversion and Management* 47 (2006) 2602-2611.

[2] Giltrap DL, McKibbin R, Barnes GRG, A steady state model of gas-char reactions in a downdraft biomass gasifier, *Solar Energy* 74 (2003) 85-91.

[3] Zainal ZA, Ali R, Lean CH, Seetharamu KN, Prediction of performance of a downdraft gasifier using equilibrium modeling for different biomass materials, *Energy Conversion and Management* 42 (2001) 1499-1515.

[4] Huang, HJ, Ramaswamy S, Modeling Biomass Gasification Using Thermodynamic Equilibrium Approach, *Applied Biochemistry and Biotechnology* 154 (2009) 14-25.

[5] Melgar A, Perez JF, Laget H, Horillo A, Thermochemical equilibrium modelling of a gasifying process, *Energy Conversion and Management* 48 (2007) 59-67.

[6] Jarungthammachote S, Dutta A, Thermodynamic equilibrium model and second law analysis of a downdraft waste gasifier, *Energy* 32 (2007) 1660-1669.

[7] Ratnadhariya JK, Channiwala SA, Parametric sensitivity of downdraft gasifier as predicted bt three zone KF model, in *Proceedings of the International Conference on Mechanical Engineering 2003 Bangladesh* (2003).

[8] Sharma AK, Modeling and simulation of a downdraft biomass gasifier 1. Model development and validation, *Energy Conversion and Management* 52 (2011) 1386-1396.

[9] Roy PC, Datta A, Chakraborty N, Modelling of a downdraft biomass gasifier with finite rate kinetics in the reduction zone, *International Journal of Energy Research* 33 (2009) 833-851.

[10] Roy PC, Datta A, Chakraborty N, Assessment of cow dung as a supplementary fuel in a downdraft biomass gasifier, *Renewable Energy* 35 (2010) 379-386.

[11] Sharma AK, Equilibrium and kinetic modeling of char reduction reactions in a downdraft biomass gasifier: A comparison, *Solar Energy* 82 (2008) 918-928.

[12] Johansson R, Thunman H, Leckner B, Sensitivity Analysis of a Fixed Bed Combustion Model, *Energy & Fuels* 21 (2007) 1493-1503.

[13] Zhou H, Jensen AD, Glarborg P, Jensen PA, Kavaliauskas A, Numerical modeling of straw combustion in a fixed bed, *Fuel* 84 (2005) 389-403.

[14] Turns SR, *An introduction to combustion: concepts and applications* (2000) 2nd ed., Singapore: McGraw-Hill.

[15] Jayah TH, Aye L, Fuller RJ, Stewart DF, Computer simulation of a downdraft wood gasifier for tea drying, *Biomass and Bioenergy* 25 (2003) 459-469.

[16] Wang Y, Kinoshita CM, Kinetic model of biomass gasification, *Solar Energy* 51 (1993) 19-25.

